Upregulation of microRNA-96 alleviates the neurological damage in acute seizure rats by down-regulating RAC1 and inhibiting the activation of RhoA/ROCK signaling pathway

Zhihan Wang
Shanghai Pudong Hospital
Wei Jiang
Fudan University Shanghai Cancer Center Minhang Branch Hospital
Dabin Ren
Shanghai Pudong New area People's Hospital
Wei Chen
Shanghai pudong new area people's Hospital
Ping Zheng (jojo_ras@126.com)
Shanghai Pudong New area People's Hospital https://orcid.org/0000-0002-3928-3875

Research

Keywords: microRNA-96; Epilepsy; RAC1; RhoA/ROCK pathway; Neurological damage; Oxidative stress

Posted Date: December 18th, 2019

DOI: https://doi.org/10.21203/rs.2.19156/v1

Abstract

Objective

Today, the research about the involvement of non-coding RNAs on neurological disorders is still scarce. Hence, we aimed to investigate the effect of miR-96 targeted RAC1 to mediate RhoA/ROCK signaling pathway in neurological damage in acute seizure rats.

Methods

The acute seizure rat model was constructed by using classical chlorinated-pilocarpine injection, which was treated with miR-96 mimics, RAC1-siRNA or their controls. The number of BrdU positive cells, neuronal changes and apoptosis, expression of NGF, BDNF and GFAP were detected by different staining assays. At the same time, the activity of SOD, the content of MDA and the protein contents of TNF-α and IL-6 in rat hippocampus were detected as well. Next, the expression of NGF, BDNF, GFAP, Bax, Bcl-2, caspase-3, RAC1, RhoA and ROCK were determined by RT-qPCR and western blot analysis. Then, the binding site between miR-96 and RAC1 was analyzed by bioinformatics software and luciferase assay. Finally, the altered expression of miRNAs was investigated in exosomes released from excitotoxic neurons with a customized rat miRNA chipset.

Results

After upregulation of miR-96 or downregulation RAC1, BrdU-positive cells, TUNEL-positive cells, NGF, GFAP, MDA, TNF-α, IL-6, Bax, caspase-3, and pathway related proteins in rat hippocampus decreased while Bcl-2, BDNF, and the activity of SOD increased. Furthermore, RAC1 was found to be the target gene of miR-96 and their relationship was validated in in-vitro studies. Finally, the decreased expression of miR-96 in exosomes from kainic acid treated neurons was identified as well.

Conclusion

This study suggests that upregulation of miR-96 could downregulate RAC1 and inhibit the activation of RhoA/ROCK signaling pathway, thus alleviated the neurological damage in acute seizure rats.

Introduction

Epilepsy is a common neurologic disorder of the brain featuring by a lasting predisposition to evolve into epileptic seizures, which always having two gratuitous seizures > 24 h apart [1]. In most countries, 1.5–5% of any population would undergo nonfebrile seizures at some time, and the prevalence of epilepsy is higher in resource-needy countries, especially in rural areas [2]. Epilepsy could damage the brain, especially during development period, and is usually related to cognitive, behavioral, and psychiatric comorbidities that could severely impair quality of life [3]. Changes in the extracellular environment surrounding hippocampal neurons would result in epileptogenesis [4]. Patients with epilepsy show resistance to antiepileptic drugs (AEDs) in at least 25–30% of the cases, and its etiology still remains uncertain[5]. Although a series of studies have investigated the chronic epilepsy, there are few studies on acute seizure stage, which may have interfered in chronic epilepsy and kinds of biomarkers to specific neuronal proteins are lacking in patients with epilepsy [6].

microRNAs (miRNAs) belong to non-coding RNA with a length of 20–22 nucleotides, and are broadly distributed in various kinds of organisms [7]. They function as post-transcriptional regulators by binding to target mRNA transcripts leading to translational repression or target degradation and gene silencing [8]. Recently, dysregulation of miRNAs has gained great attention in epilepsy, such as miR-218 and miR-204 [9]. In recent years, there are tons of researches on miR-96 mediating several diseases, such as hepatocellular carcinoma, urothelial carcinoma and breast cancer [10, 11]. Serum profiles of the miRNA of 30 epileptic patients versus 30 healthy control identified 4 miRNAs were significantly upregulated (let-7d-5p, miR-106b-5p, miR-130a-3p, and miR-146a-5p), whereas 6 miRNAs (miR-15a-5p, -144-5p, -181c-5p, -194-5p, -889-3p, and novel-mir-96) were downregulated in 2,578 serum miRNAs with the Illumina platform, and authors further validated miR-96 were most downregulated with RT-PCR [12]. RAC1, a member of the Rho family of tiny GTP-binding proteins, is reported to involve in tumorigenesis and metastasis, and its best characterized function is the cytoskeleton rearrangement [13]. The Rho GTPase RAC1 is widely recognized as a mediator in the inflammatory process of innate immune system [14]. A recent study showed that down-regulation of RAC1 reduced spontaneous seizures at the chronic stage of epilepsy, and further proved that RAC1-GTP was closely involved in the pathology of epilepsy [15]. However, authors did not further investigate the mechanism associated with decreased RAC1 in epilepsy models and the downstream pathway of RAC1 in epilepsy remains to be elucidated as well. Rho kinase (ROCK) is a serine/threonine kinase and a potential target of the small GTPase Rho, which plays a major role in central nervous system [16]. Evidence has proved that RhoA pathway, along with its downstream effector ROCK, was also involved in epilepsy [17]. In addition, miR-96 has been found to be involved in Rac1 signaling in a mouse model of inherited retinal degeneration. Both in vitro and in vivo interaction of miR-96 and Rac 1 were confirmed. They also proposed that miR-96 is involved in transmembrane transport, cell-adhesion, signal transduction and apoptosis [18]. However, there are still few profound researches on specific causative factors and mechanisms in epilepsy. Hence, the present study was performed to identify miR-96 reduced the neurological damage in acute seizure rats by down-regulating RAC1 and inhibiting the activation of RhoA/ROCK signaling pathway.

Materials And Methods

Ethics statement

This study was approved by the local Ethics Committee. All animal experiments were conformed to the Guide for the Care and Use of Laboratory Animal by local committees.

Model preparation and experiment grouping

A total of 120 clean Sprague-Dawley (SD) rats (aged 6-8 weeks, weighed 200 (200 ± 10.5) g) were selected and purchased from Beijing Vital River Laboratory Animal Technology Co., Ltd. (Chaoyang District, Beijing, China). All rats were fed in standard animal rooms with relatively quiet environment and free access to drinking water and food. The indoor temperature was (20 ± 2)°C and the humidity was (50 ± 3)%. All SD rats were fed adaptively for 7 days before the experiments.

The acute seizure rat model was constructed by using classical chlorinated-pilocarpine injection: first, lithium chloride (127 mg/kg) was injected into 100 rats through intraperitoneal (ip) injection, 12 hours later, methylatropine bromide (10 mg/kg) was injected by the same method. Thirty minutes after the onset, a dose of 100 mg/kg pilocarpine was injected ip. Diazepam (4 mg/kg), atropine (1 mg/kg) or phenobarbital (25 mg/kg) was needed when the seizure duration exceeded 1 h, or the rats were severely twitched to an endangered state. The seizure degree was determined by the Racine's score, and the model was successfully constructed if the status seizure lasted 30 min. In the normal control group, physiological saline was used instead of lithium chloride-pilocarpine, and no other different treatments with SE. The latency period was measured by behavioral observation, and the Racines' score was used to evaluate the severity of convulsions in rats (Racine, 1972) including: I, mouth and facial movement; II, head nodding; III, forelimb clonus; IV, rearing with forelimb clonus; V, rearing and falling with forelimb clonus and VI, endangered to death status.

Overexpression of miR-96 and Rac1 siRNA interference assay

miR-96 mimics (a synthetic double-stranded RNA oligonucleotide mimicking miR-96 precursor) and negative control (NC) as synthetic negative control RNAs were purchased from Ribobio (Guangzhou, China). 1 nmol miR-96 mimics or NC in 5 μl PBS was injected into the ventricle of SE insult rat using a 30-gauge needle with 5-μl Hamilton syringe injections. For in vitro studies, primary cultured neurons were seeded into 6-well plates and transfected the following day when the cells were approximately 70% confluent using Lipofectamine 2000 (Invitrogen, Carlsbad, CA, USA) according to the manufacturer's instructions. For each well, equal dose (1nmol) of miR-NC or miR-96 was added. miR-96 mimics were given at a different dose from 0 to 10 nmol. Cells were harvested 24 h after transfection, and total RNA was extracted for quantitative RT-PCR analysis and chip-assay. The Rac1 siRNA and siRNA-NC were similarly applied to cultured neurons for validation.

The Rac1 siRNA targeting human Rac1 cDNA was designed and synthesized by Ribobio (Guangzhou, China). A scrambled siRNA served as a negative control (siRNA-NC). The sequence was selected according to the following requirements: (a) the sequence was as close as possible to the designed primer region, and (b) the sequence was homologous with that of rat Rac1 mRNA. The homologous sequences between the selected siRNA sequence and other gene sequences were excluded. The sequence of the siRNA was as follows:

Forward:5'GATCCCCACAAGAAGATTATGACAGATTCAAGAGATCTGTCATAATCTTCTTGTTTTTTGGAAA3';Reverse:5'AGCTTTTCCAAAAAACAAGAAGATTATGACA
3'.

Model Treatment

Rats (n = 120) were randomly divided into 6 groups (20 in each group): normal group, status epilepsy group (SE group), miR-96 mimics negative control group (mimics NC group), miR-96 mimics group, RAC1 interference NC group (siRNA-NC group) and RAC1-siRNA group.

Within 24 hours before the establishment of SE rats, rats in the miR-96 mimics group were injected with 1 nmol (50 μL) of miR-96 mimics into the unilateral ventricle of SD rats; rats in the mimics NC group were injected with 1 nmol (50 μL) of miR-96 mimics NC; the RAC1-siRNA group were injected with 5 nmol (10 μL) of the RAC1 interference plasmid; the siRNA-NC group were injected with 5 nmol (10 μL) of the RAC1 interference NC plasmid. miR-96 mimics, mimics NC, RAC1-siRNA, and siRNA-NC were purchased from Ribo Biotechnology Co., Ltd. (Guangzhou, China).

Electroencephalogram recording

Rats with grade III or higher seizure stages lasting three hours were included in the following study according to the criteria for classic seizures. Three hours after the seizure, two epileptic rats were randomly selected from each group and electroencephalography was performed. The acute seizure rats were first anesthetized with 10% hydrated chloric acid (0.35 ml/kg) by intraperitoneal administration (i.p.), then the anesthetized rats were fixed with a locator, and brain electrical activity was recorded by using three leads. Needle electrodes were placed in the bilateral cerebral cortex and hippocampus with a diameter of 0.5 mm. All electrodes were fixed with dental powder and 502 glue. RM6240B multi-channel physiological recorder was used for recording (Shanghai Gongyi, China). Paper speed: 30 mm/s.

Collection of brain tissue in rats

After 3 hours of modeling, 5 SD rats were randomly taken from each group and brain tissue was collected as previously reported [10,17]. Paraformaldehyde PB solution was perfused and used for fixing when the liver was observed turning from red to white, the saline outflow from right heart auricular turning colorless. The brain tissues were then placed in 4% paraformaldehyde PB solution for fixing overnight. Paraffin sections were routinely prepared for hematoxylin-eosin (HE) staining and immunohistochemical staining. In other group, 5 rats were randomly selected and immediately decapitated, and the bilateral hippocampus were quickly removed. One side was stored in a -80°C refrigerator for enzymatic detection, and the other side was fixed in 3% glutaraldehyde for about 5 min. After that, the hippocampus was trimmed into 1 mm^3 pieces to prepare the electron microscope specimen.

BrdU labeling and immunofluorescence staining

After 3 hours of modeling, 3 SD rats were randomly selected from each group, and BrdU (100 mg/kg) was intraperitoneally injected within 24 hours after the last related operation, and the brain tissues was perfused according to the above steps 24 hours after injection. The obtained brain tissues were fixed in 4%

paraformaldehyde for 24 hours. After the fixation, the brain tissues were placed in PB solution (containing 10% - 20% sucrose) overnight (4°C) until the bottom was sedimented. After that, the sample was taken out in the coronal position, and 1 to 2 mm^3 hippocampus tissues were taken and 5% agar was used to make a concentration of 0.01 mol/L phosphate buffer saline (PBS). The prepared agar was used to fix the hippocampus tissue section, and each piece was continuously taken for 10 pieces with a thickness of about 50 μm.

The hippocampal tissue of each group was washed with PBS for 10 min × 3 times. The antigen was repaired by 2N-Cl (37°C, 30 min), followed by 0.1 mol/L boric acid buffer (pH 8.5) rinsing for 10 min. Then, BrdU (1:300, Abcam, Cambridge, MA, USA) was added with 0.01 mol/L fetal bovine serum (BSA)-PBS, placed in a refrigerator (4°C, overnight), and then rinsed with PBS (10 min, 3 times). After that, 0.01 mol/L BSA-PBS was added to Cy3 monkey anti-rat IgG (1:200) and incubated (1 h, room temperature), rinsed with PBS, and glycerin was used for sealing. After that, the sections were placed under a laser confocal microscope, and observed from the X, Y, and Z axis, and the number of BrdU-positive cells was recorded. Images were processed by Image J (Oxford UK).

HE staining

The prepared paraffin sections were routinely dewaxed to water, then hematoxylin was used for staining (10 min). Then 1% hydrochloric acid was used to separate color (2 - 5 s), followed by ammonium hydroxide for returning blue (20 - 30 s), and eosin was added for staining (5 min). After rinsing (3 min), gradient alcohol was used for color separation followed by regular dehydration and clearance, then neutral gum was taken for sealing, and finally microscope (Nikon, Tokyo, Japan) was used for observation.

Electron microscopy specimen preparation and observation

The obtained diced tissues were fixed in 3% glutaraldehyde for 3 h, and rinsed with PBS. Subsequently, the diced tissues were fixed with 1% of osmic acid for 2 h, followed by dehydration with gradient alcohol, and resin was used to embed the tissues. Then, the LKBIII ultrathin slicer (Pharmacia LKB, Sweden) was used for sectioning, and double-electron staining by uranyl acetate and lead citrate, and observed with JE-OLJEM-2100F transmission electron microscope (Siemens, Berlin, Germany).

Toluidine blue staining

The above-mentioned hippocampal tissue was placed in xylene and immersed in gradient ethanol. Then, it was stained with 1% toluidine blue (40 min). After that, the color separation was performed, and sections were cleared by using xylene and gradient alcohol, and then sealed with a neutral gum. Finally, a microscope (Nikon, Tokyo, Japan) was used to count and analyze the Nissl positive cells.

TdT-mediated dUTP Nick-End Labeling (TUNEL) staining

The above-mentioned hippocampal tissues were detached in proteinase K (1 h, room temperature). Then, the tissue was routinely treated by the TUNEL reaction kit. Finally, the apoptotic cells' number were recorded under a microscope (Nikon, Tokyo, Japan). TUNEL staining was used for staining positive cells and its color turned brown yellow or brown.

Immunohistochemical staining

The prepared paraffin tissue sections were baked at room temperature for 60 min. After conventional xylene dewaxing and alcohol hydration, 0.3% fresh hydrogen peroxide solution (H_2O_2) was prepared and sealed the tissue for 5-10 min. Next, sections were immersed in 0.01 mol/L citrate buffer (pH 6.0, 95°C), and the sections were heated for 10-15 min. After cooling, 5% goat serum was added (30 min, room temperature) followed by primary anti-nerve growth factor (NGF) (1:200, Millipore, Inc., Massachusetts, USA), brain-derived neurotrophic factor (BDNF) (1:500, Abcam, Cambridge, MA, USA), and glial fibrillary acidic protein (GFAP) (1:1000, Abcam, Cambridge, MA, USA) were added. Then the sections were incubated (2 h, 37°C) and placed overnight (4°C). According to the kit instructions, the corresponding secondary antibody was added, and together with the horseradish-labeled streptavidin incubated (2 h, 37°C). Finally, the diaminobenzidine (DAB) coloring solution was used for color development (The normal group was not added with primary antibody, replaced with 0.01 mol/L PBS, and the other steps were the same). Each immunohistochemical stained section was quantitatively analyzed by Image Pro Plus 6.0 image. Three fields of view were casually chosen for each measurement, and the average value was taken. At the same time, the number of NGF, BDNF, and GFAP immunoreactive cells was also observed.

Spectrophotometry detection

The hippocampal tissues were added with saline in a ratio of 1:9 to make a 10% brain tissue homogenate on ice. Subsequently, it was centrifuged (15 min, 4°C, 3000 r/min), and the supernatant was collected. After that, the activity of superoxide dismutase (SOD) and malonadialdehyde (MDA) were determined by chemical colorimetry based on the instructions of detection kit (Nanjing JianCheng Bioengineering Institute, Nanjing, China).

Enzyme-linked immunosorbent assay (ELISA)

According to the instruction of ELISA kit (Yixin Bioengineering Co., Ltd., Shanghai, China), the homogenate supernatant was assayed for measuring tumor necrosis factor-α (TNF-α) and interleukin-6 (IL-6). The steps were as follows: first, the 50 μL coated antibody was added to each well, then incubated at 4°C. After that, the plate was washed with a washing solution, then 150 μL of blocking solution was poured into each well, and the plate was washed at 37 °C for 1 h. After a standard curve was established, 50 μL of the sample was added and mixed at room temperature (2 h). Subsequently, avidin was added to each well, and the tetramethyl benzidine (TMB) substrate working solution was poured into each well. The reaction was performed in the dark (room temperature, 10 min). Finally, H_2SO_4 (2M) was added to each well to stop the liquid mixture. The microplate reader was used to measure the absorbance at 450 nm and 405 nm, respectively, and the concentration value was obtained by calibration.

Reverse transcription quantitative polymerase chain reaction (RT-qPCR)

Total RNA from brain tissues were extracted with a one-step method from Trizol (Invitrogen, Carlsbad, CA, USA). Optical density (OD) and RNA concentrations were determined by ultraviolet spectrophotometry. miR-96 was subjected to Poly(A) tailing reaction and reverse transcription reaction by using the One Step PrimeScript ® miRNA cDNA Synthesis Kit (Perfect Real Time) reverse transcription kit from TaKaRa (Bio, Inc., Shiga, Japan). The mRNA was subjected to a reverse transcription reaction by using a TaKaRa PrimeScript® RT reagent Kit (Perfect Real Time) reverse transcription kit. PCR forward and reverse primers were invented and synthesized by Invitrogen (Invitrogen, Carlsbad, CA, USA) (Table 1). RT-qPCR was performed by using SYBR Green chimeric fluorescence. The PCR reaction was performed by using SYBR Premix Ex Taq (Perfect Real Time) kit reagent. U6 worked as an internal reference for miR-96, and glyceraldehyde-3-phosphate dehydrogenase (GAPDH) played an internal reference role in concerning NGF, BDNF, GFAP, Bax, Bcl-2, caspase-3, TNF-α, IL-6, RAC1, RhoA, and ROCK mRNA. $2^{-\triangle\triangle Ct}$ was used to obtain the relative expression level of the target gene [19] . The experiment was performed three times.

Western blot assay

The total protein in the hippocampus was extracted, and the bicinchoninic acid protein concentration determination kit (Beyotime Biotechnology Research Institute, Shanghai, China) was used to determine the protein concentration, and the concentration of all group was adjusted uniformly. The total protein from each group was added with 80 μL 5× sodium dodecyl sulfate (SDS) protein loading buffer, and the protein was degenerated by boiling water for 5 min. After the transfer was completed, the polyvinylidene difluoride (PVDF) membrane was removed and placed in 5 mL blocking solution (room temperature, 1 h). Primary antibody: NGF, GAPDH (1:400 and 1:1000 respectively, Millipore, Massachusetts, USA), BDNF, GFAP, Bax, Bcl-2, RAC1 (1:1000, Abcam, Cambridge, MA, USA), caspase-3, RhoA, ROCK (1:500, 1:5000, 1:2000, respectively, Abcam, Cambridge, MA, USA) were added, and incubated overnight (4°C). The corresponding secondary antibody was added after washing the membrane, then incubated (1 h, room temperature). The PVDF membrane was reacted with the chemiluminescent substrate of the hypersensitive ECL luminescence reagent. The blot strip was imaged by Image J. Gray value analysis was done, and GAPDH worked as an internal reference to analyze the expression of NGF, BDNF, GFAP, Bax, Bcl-2, caspase-3, RAC1, RhoA and ROCK proteins in all groups.

Luciferase activity assay

The target site of RAC1 and corresponding miR-96 binding was determined by online prediction software http://www.targetscan.org, and the primers were designed with the 3'-untranslated region (3'UTR) sequence of RAC1 gene. We also performed a PCR chip array (designed by WCgene Biotech, Shanghai, China) to obtain the top 10 target genes of miR-96. We compared the expression of different genes targeted by miR-96 mimics against the negative control and listed the top ten decreased genes. The forward and reverse primers were introduced into restriction endonuclease Hind III and Spe I. The mutated sequence of the binding site was designed, and the target sequence fragment was synthesized by Nanjing Genscript Biotechnology Co., Ltd. (Nanjing, China). The amplified target product and the pMIR-REPORT^{TM} Luciferase vector plasmid were digested with restriction endonuclease Hind III and Spe I, and the digested product was recovered, and ligated with T4 DNA ligase to transform Escherichia coli DH5α competent cells. The correct recombinant plasmid was identified by enzyme digestion and sequenced. In a 24-well plate, 1 × 10^5 PC12 cells were seeded into each well. The cells were co-transfected with the recombinant plasmid and miR-96 mimics (48 h). The cell culture medium was discarded and washed 3 times with PBS. After lysis of the cell lysate 100 uL of the luciferase kit for 30 min, 20 uL of cell lysate was taken and 100 uL of LARII was added, the fluorescence value (A) was measured, 100 uL of Stop&Glo reagent was added, the fluorescence value (B) was measured. The fluorescence value (A) worked as an internal reference, and the luciferase activity value C = B/A .

Exosomes isolation from cell cultures and NTA analysis

Cortical cultures were obtained from either E18 or P3 rat (P3 days for astrocytes and E18 for neurons) as previously reported [19]. The cultured medium from four groups Q1~Q4 were collected and stored in 4℃ fridge.

Exosome Isolation: The supernatant of cell medium was taken from the 4°C freezer, balanced with PBS, and centrifuged at 1500g, 4°C for 30 minutes; the supernatant was taken and for a next 10000g, 4 ° C, centrifugation for 60 minutes; after this, the supernatant was centrifuged again at 12000g, 4 ° C for 30 minutes; Next, the centrifugated supernatant was carefully moved to a single-use ultracentrifugation, at 110000g for 60 minute at 4°C; carefully discard the supernatant after centrifugation, and the trace liquid at the bottom of the obtained centrifuge tube is exosomes. Carefully blow the bottom of the centrifuge tube with 30-100 ul volume of 1×PBS and inhale into 0.5- 1.5 ml centrifuge tube, gently pipet with a pipette to completely dissolve.

For the Transmission electron microscopy morphology investigation, 10 ml of exosomes pellet was placed on formvar carbon-coated 200-mesh copper electron microscopy grids, and incubated for 5 min at room temperature, and then was subjected to standard 1% uranyl acetate

staining for 1 min at RT. The grid was washed with three times of PBS and allowed to semi-dry at room temperature before observation in transmission electron microscope (Hitachi H7500 TEM, Japan).

Analysis of absolute size distribution and concentration of exosomes were determined using Nanoparticle tracking analysis (NTA). Exosomes were diluted in 1ml PBS and mixed well, then the diluted exosomes were injected into the NanoSight NS300 instrument (Malvern, UK), particles were automatically tracked and sized based on Brownian motion and the diffusion coefficient. Filtered PBS was used as controls. The NTA measurement conditions 25 frames per second, measurement time 60s. The detection threshold was similar in all the samples. Three recordings were performed for each sample.

MiRNA quantitative RT-PCR (qRT-PCR) array

The miRNA qRT-PCR array experiments were conducted at Wcgene Biotechnology Corporation, Shanghai. Total RNAs, including miRNAs, were isolated from 100 μl of liquid sample, using a 1-step acidified phenol/chloroform purification protocol. Synthesized exogenous RNAs were spiked into each sample to control for variability in the RNA extraction and purification procedures. The purified RNAs were polyadenylated through a poly(A) polymerase reaction and

was then reversed-transcribed into cDNA. Individual miRNAs were quantified in real-time SYBR Green RT-qPCR reactions with the specific MystiCq miRNA qPCR Assay Primers (Sigma-Aldrich). The protocol of miRNA qRT-PCR array analysis was as described in detail on the website of Wcgene (http://www.wcgene.com).

Statistical analysis

All the data were processed by SPSS 21.0 statistical software (IBM Corp. Armonk, NY, USA). The measurement data were showed in the form of mean ± standard deviation. The data with normal distribution between pairwise groups were conducted by the t test and one-way analysis of variance (ANOVA) was used for comparison among various groups. The least significant difference (LSD) test was taken for pairwise comparison. $P < 0.05$ indicated the difference was statistically significant.

Results

Modeling of acute seizure

After introduction of lithium chloride-pilocarpine in rats, we found that: after injection of pilocarpine for 5-30 min, acute seizure rats began to behave mechanical chewing, continuous nodding, unilateral forelimb clonic, and alternate clonus of forelimb. After that, there were bilateral forelimbs clonus, retreats, falls, and finally the rats began screaming and running, reaching the state of spasticity. 12-15 SD rats in the SE group, mimics NC group, siRNA-NC, miR-96 mimics and siRNA-RAC1 groups were successfully induced, and the successful rate was about 60-75%. SE indicated level III or above.

Upregulated miR-96 or silenced RAC1 reduces Racine score and prolongs latency of epilepsy in rats

The Racine scores of SD rats in each group within 3 hours were (Fig. 1A): facial clonus + rhythmic nodding + forelimb clonus + hind limb standing scored 4 points, facial clonus + rhythmic nodding + forelimb clonus + hind limb standing + falling scored 5 points, accompanied by hoarseness and galloping scored 6 points, spasticity scored 7 points. No significant difference in Racine scores was found among the SE, mimics NC and siRNA-NC groups ($P > 0.05$). Compared with the mimics NC group, the Racine score of the miR-96 mimics group was lower ($P < 0.05$); in contrast to the siRNA-NC group, the Racine score of the siRNA-RAC1 group was also lower ($P < 0.05$).

Considering the latency of each group of rats, we found (Fig. 1B) that the average latency period of the SE group was 50.15 ± 2.32 minutes. If taken SE group as the comparison group, there was no obvious difference in latency period compared with the mimics NC group (50.55 ± 2.12 min) and the siRNA-NC group (50.12 ± 2.42 min) ($P > 0.05$). In contrast to the mimics NC group, the latency period of the miR-96 mimics group (58.98 ± 2.45 min) was prolonged ($P < 0.05$); compared with the siRNA-NC group, the latency period of the siRNA-RAC1 group (57.32 ± 3.82 min) was stretched as well ($P < 0.05$).

Upregulated miR-96 or silenced RAC1 reduces the high amplitude spike wave and frequency of electroencephalogram (EEG)

The EEG of rats in each group was monitored. We found (Fig. 2) that in the normal group, all rats mainly showed α wave and β wave, the basic wave scattered in a small amount of θ wave, and no seizure wave was released. High amplitude spikes were observed in the SE, mimics NC and siRNA-NC groups. The amplitude and frequency of spikes in the miR-96 mimics group were dramatically lower than those in the mimics NC group, which in the siRNA-RAC1 group were obviously lower than those in the siRNA-NC group.

Upregulated miR-96 or silenced RAC1 significantly reduces BrdU-positive cells

The BrdU-positive cells was detected by BrdU labeling and immunofluorescence staining. We found (Fig. 3) that the number of BrdU-positive cells in the normal group was 20.33 ± 2.35. In contrast to the normal group, the number of BrdU positive cells in the SE group (35.42 ± 2.75) increased ($P < 0.05$). In contrast to the SE group, no obvious difference in the number of BrdU positive cells between the mimics NC group (35.87 ± 2.05) and the siRNA-NC group (35.52 ± 2.45) ($P > 0.05$); in contrast to the mimics NC group, the number of BrdU positive cells in the miR-96 mimics group (25.58 ± 3.22) decreased dramatically ($P < 0.05$). Compared with the siRNA-NC group, the number of BrdU-positive cells in the siRNA-RAC1 group (26.08 ±3.12) was also obviously reduced ($P < 0.05$).

Upregulated miR-96 or silenced RAC1 inhibit the pathological changes of hippocampus in acute seizure rats

For HE staining, we found (Fig. 4A) that the hippocampal tissues of SD rats in all group were homogeneously stained, the neurons in the normal group were well-organized, well-arranged, with clear layers and clear nuclei. In contrast to the normal group, the SE group showed uneven staining, severe degeneration, shrinkage and loss of a great number of neurons, extensive loose tissue edema, with a great number of vacuoles, disordered arrangement of remaining neurons and unclear hierarchy. The morphological structure of hippocampus was similar in the SE group, mimics NC group and siRNA-NC group. The hippocampal neuronal condition in the miR-96 mimics group and siRNA-RAC1 group was between the SE group and the normal group. Some neurons showed pyknosis, the vacuole area narrowed, the cell arrangement was slightly disordered, the layers were still identifiable, and most of the nuclei were clear.

The ultrastructure of hippocampal tissue of SD rats in each group was observed by an electron microscopy. We found (Fig. 4B) that the structure of hippocampal neurons in the normal group was basically normal with complete morphology, clear outline and boundary. There was no decrease in the number of neurons, no deformation or necrosis. In the SE group, the hippocampal structure was obviously damaged, with obvious cell swelling, incomplete cell morphology, blurred outline, unclear boundaries, disordered arrangement, cell deformation, necrosis and neuronal reduction. The morphological structure of hippocampal neurons in the SE group, mimics NC group and siRNA-NC group was similar. The hippocampal tissues of the miR-96 mimics group and siRNA-

RAC1 group showed mild edema in cytoplasm and nucleus of neurons. The number of organelles decreased, the proliferation degree was lighter, the number of cell ruptures was less, the shape was more complete, the outline and boundary were clearer, the arrangement was more orderly, the deformation and necrosis of neurons were lighter, and the neuron did not decrease dramatically.

After Nissl's staining, we found (Fig. 4C): In the hippocampus of the normal group, most cell were survived. In the SE group, mimics NC group and siRNA-NC group, pyramidal cells were obviously disordered, and survival neurons decreased. The morphology and staining of hippocampal neurons in the miR-96 mimics and the siRNA-RAC1 groups were similar to those in the normal group. The number of hippocampal neurons decreased in SE group compared to control group, with a similar reduced trend in SE group with miRNA-96 NC and siRNA NC group (Fig. 4D). In contrast to the mimics NC group, the number of Nissl positive cells in the miR-96 mimics group increased. In contrast to the siRNA-NC group, the number of Nissl positive cells in the siRNA-RAC1 group also increased ($P < 0.05$).

Upregulated miR-96 or silenced RAC1 reduces TUNEL-positive cells, inhibits Bax and caspase-3, and promotes Bcl-2 in acute seizure rats

TNUEL assay was used to detect apoptosis in hippocampus of SD rats in each group. We found (Fig. 5A) that the number of TUNEL positive cells in the SE group increased in contrast to that in the normal group ($P < 0.05$). In contrast to the SE group, there was no obvious disparity in the number of TUNEL positive cells between the mimics NC group and siRNA-NC group ($P > 0.05$). In contrast to the mimics NC group, the number of TUNEL positive cells in the miR-96 mimics group decreased. In contrast to the siRNA-NC group, the number of TUNEL positive cells in the siRNA-RAC1 group decreased ($P < 0.05$).

The Bax, caspase-3 and Bcl-2 expression in the hippocampus of SD rats in all group was determined by RT-qPCR and western blot analysis. We found (Fig. 5B, C) that Bax and caspase-3 expression in the SE group was higher than that in the normal group, while the expression of Bcl-2 in the SE group was lower than that in the normal group (all $P < 0.05$). No obvious disparity was found in Bax, caspase-3, Bcl-2 expression among the SE, mimics NC and siRNA-NC groups ($P > 0.05$). Compared with the mimics NC group, Bax and caspase-3 expression levels decreased and Bcl-2 level increased in the miR-96 mimics group ($P < 0.05$); compared with the siRNA-NC group, Bax and caspase-3 expression levels decreased in the siRNA-RAC1 group, while Bcl-2 level increased ($P < 0.05$).

Upregulated miR-96 or silenced RAC1 inhibits NGF and promotes BDNF expression in acute seizure rats

NGF and BDNF expression in hippocampus of SD rats in all group were determined by immunohistochemical staining. We found (Fig. 6A, B): the number of positive cells of NGF and BDNF in the SE group increased compared with normal group. ($P < 0.05$). In contrast to the SE group, no significant difference in the number of NGF and BDNF positive cells found in the mimics NC group and the siRNA-NC group ($P > 0.05$). Compared with the mimics NC group, the number of positive cells of NGF was decreased in the miR-96 mimics group, and the number of positive cells of BDNF was increased ($P < 0.05$). In contrast to the siRNA-NC group, NGF-positive cells number in the siRNA-RAC1 group decreased, and the number of BDNF-positive cells increased ($P < 0.05$).

The expression of NGF and BDNF in hippocampus of SD rats in each group were determined further by RT-qPCR and western blot analysis. We found (Fig. 6C, D): NGF and BDNF expression increased in the SE group compared with normal group ($P < 0.05$). No dramatic difference in the expression of NGF and BDNF was found among the SE group, the mimics NC group and the siRNA-NC group ($P > 0.05$). In contrast to the mimics NC group, the expression of NGF in the miR-96 mimics group decreased, and BDNF expression increased ($P < 0.05$). In contrast to the siRNA-NC group, the NGF expression in the siRNA-RAC1 group was decreased, and the BDNF expression increased ($P < 0.05$).

Upregulated miR-96 or silenced RAC1 inhibits GFAP expression in acute seizure rats

The expression of GFAP in hippocampus of SD rats in all group were detected by immunohistochemical staining (Fig: 7A), RT-qPCR and western blot analysis (Fig. 7B, C). We discovered that GFAP expression in hippocampus of the SE group was higher than that in the normal group ($P < 0.05$). Compared with the SE group, GFAP expression in hippocampus of rats in the mimics NC group and siRNA-NC group had no obvious difference ($P > 0.05$). In contrast to the mimics NC group, the expression of GFAP in hippocampus of the miR-96 mimics group decreased ($P < 0.05$). Compared with the siRNA-NC group, GFAP expression in hippocampus of rats in the siRNA-RAC1 group also decreased ($P < 0.05$).

Upregulated miR-96 or silenced RAC1 increases SOD activity and decreases MDA content in acute seizure rats

The SOD activity and MDA content in hippocampus of rats in each group were tested. We found (Fig. 8A, B) that compared with the normal group, SOD activity in the SE group decreased and MDA content increased ($P < 0.05$). In contrast to the SE group, no major difference was found in SOD activity and MDA content between the mimics NC group and siRNA-NC group ($P > 0.05$). Compared with the mimics NC group, SOD activity increased, and MDA content decreased in the miR-96 mimics group ($P < 0.05$); compared with the siRNA-NC group, SOD activity also increased and MDA content decreased in the siRNA-RAC1 group ($P < 0.05$).

Upregulated miR-96 or silenced RAC1 inhibits TNF-α and IL-6 expression levels in acute seizure rats

TNF-α and IL-6 expression in hippocampal homogenate of rats in all group was detected by RT-qPCR and ELISA. We found (Fig. 9A, B) that TNF-α and IL-6 expression was low in the normal group. Compared with the normal group, TNF-α and IL-6 levels in the SE group were higher ($P < 0.05$). In contrast to the SE group, the levels of TNF-α and IL-6 in the mimics NC group and siRNA-NC group had no obvious difference ($P > 0.05$). Compared with the mimics NC group, the levels of TNF-α and IL-6 in the miR-96 mimics group decreased ($P < 0.05$). Compared with the siRNA-NC group, the levels of TNF-α and IL-6 in the siRNA-RAC1 group were also lower ($P < 0.05$).

Upregulated miR-96 or silenced RAC1 inhibits RhoA and ROCK expression levels in acute seizure rats

RT-qPCR was used to detect the expression of miR-96 in hippocampus of rats in each group. We found (Fig. 10A): In contrast to the normal group, miR-96 expression level in the SE group decreased, suggesting that the expression of miR-96 was down-regulated in SE rats ($P < 0.05$). Compared with the SE group, no major disparity in miR-96 expression between the mimics NC group and siRNA-NC group ($P > 0.05$). In contrast to the mimics NC group, miR-96 expression level of the mimics group increased ($P < 0.05$). Compared with the siRNA-NC group, no dramatic change in miR-96 expression level in the siRNA-RAC1 group ($P > 0.05$).

RT-qPCR and western blot analysis were applied to determine the expression of RAC1, RhoA and ROCK in hippocampus of each group. We found (Fig. 10B) that RAC1, RhoA, and ROCK expression levels were increased in the SE group compared with the normal group. In contrast to the SE group, mimics NC group and siRNA-NC group had no dramatic difference in ROCK, RAC1 and RhoA expression ($P > 0.05$). In contrast to the mimics NC group, RAC1, RhoA and ROCK expression levels in the miR-96 mimics group decreased (all $P < 0.05$). In contrast to the siRNA-NC group, the expression levels of RAC1, RhoA and ROCK in the siRNA-RAC1 group also decreased (all $P < 0.05$).

RAC1 is a direct target gene of miR-96

Target Scan was used to recognize the target sites of RAC1 binding to corresponding miR-96, and the sequence of 3'-UTR of RAC1 binding to miR-96 was shown in Fig. 11A. By using luciferase activity detection (Fig. 11B), we co-transfected the recombinant plasmids of miR-96 mimics and Wt-miR-96/RAC1 or Mut-miR-96/RAC1 in PC12 cells. The results indicated that the luciferase activity of Mut-miR-96/RAC1 was not dramatically affected by miR-96 mimics, but the luciferase activity of Wt-miR-96/RAC1 was obviously decreased ($P < 0.05$). We also confirmed the up-regulation of miR-96 and down-regulation of Rac1 after miR-96 mimic or Rac1 siRNA treating in primary cultured neurons (Fig. 11C). Based on the target prediction from Targetscan, we did a PCR array for selected targets of miR-96. Then, we analyzed their expression based on the weight and selected top 10 genes shown in the bubble figure (Fig. 11D). Next, we confirmed the dose-dependent relationship between miR-96 mimic and relative expression of Rac1. With the increased concentration of miR-96, the Rac1 expression decreased gradually with a linear relation (R square=0.6108 and $P < 0.05$).

Decreased expression of miR96 in exosomes released from excitotoxic neurons

To investigate the mechanism that downregulation of miR-96 in epilepsy, we applied a customized rat miRNA chipset to explore the miRNA alterations in exosomes from excitotoxic neurons. We found 57 miRNAs increased in exosomes from excitotoxic neurons treated with Kainic acid, and 47 miRNAs decreased their expression when co-cultured with astrocytes, while 41 had this increased-decreased pattern as shown in Figure 12. In this case, we looked at the expression of miR96, which was decreased in KA treated neurons and the co-cultured astrocytes could increase its expression.

Discussion

About 20%-40% of patients with epilepsy are refractory to medical treatment, presurgical evaluation for these patients including detailed history and examination, video electroencephalography (EEG) telemetry, advanced epilepsy protocol magnetic resonance imaging (MRI) researches, and neuropsychological and psychiatric evaluation [20]. The most common type of epilepsy is temporal lobe epilepsy (TLE), neuropsychological impairments in adult patients with TLE include deficits in a wide range of cognitive dysfunction and psychological disorders [21]. In the study, we determined to focus on the effect of miR-96 in acute seizure rats. We found that miR-96 alleviated the neurological damage in these rats by down-regulating RAC1 and inhibiting the activation of RhoA/ROCK signaling pathway.

First, we learned that miR-96 was down-regulated in SE rats, and up-regulation of miR-96 inhibited the pathological changes of hippocampus in acute seizure rats. Small noncoding RNAs, namely miRNAs, exert their functions in epileptogenesis, with potential contributions by acting as valuable biomarkers and targets for epilepsy therapy [22]. Consistent with our study that autophagy-related miR-96 was down-regulated in the hippocampus of SE rats, and SE-induced brain injury was attenuated by up-regulating miR-96 [23]. Also, it has been proved miR-96 was down-regulated in pancreatic cancer [24], and over-expression of miR-96 in pancreatic cancer inhibited cell proliferation, migration and invasion [25]. In addition, we found that RAC1 was upregulated in SE rats. Also, a recent study has shown increased expression of RAC1 in epilepsy patients and animal models [15]. Still, RAC1 expression is also up-regulated in testicular, gastric, breast and oral squamous cell carcinoma and plays a significant role in cell proliferation and tumor survival in vitro [26]. Furthermore, RAC1 has been found to be activated during muscle contraction in murine and human skeletal muscle [27], and it owns the capacity of stimulating actin cytoskeleton reorganization [28]. Additionally, we found that RAC1 was a direct target gene of miR-96 and it remained at the top of target genes after miR-96 mimics treatment. Evidence has suggested that RAC1 was co-regulated by miR-182 and miR-96 in the mouse retina [29]. Furthermore, we also found that upregulation of miR-96 could downregulate RAC1 and inhibit the activation of RhoA/ROCK signaling pathway. Inhibition of RAC1 is suggested to contribute to the Rho/ROCK-mediated maintenance of Cdc42-dependent protrusion [30].

BrdU often incorporates into denovo-synthesized DNA as the replacement for thymidine and hence permanently labels proliferation and daughter cells until it is diluted out through several rounds of cell division [31]. Increased BrdU-positive cells were found in acute seizure rats of our experiment. Consistently, there is an increase in BrdU-positive cells in the hippocampus of neonatal mouse in the injured area [32]. Antiapoptotic B-cell lymphoma 2 family members Bcl-2 is introduced to inhibit autophagy, also block the proapoptotic activity of Bcl-2-associated Bax and Bcl-2 homologous antagonist/killer, and plenty of inducers of autophagy cause cell death [33]. Caspase-3, an executioner caspase, lies downstream of both extrinsic and intrinsic (mitochondrial) pathways of apoptosis, which plays a dominant role in programmed cell death of various cell types, including neurons [34]. In our experiment, increased Bax, caspase-3, and decreased Bcl-2 were discovered in acute seizure rats. It has been suggested that epilepsy induces an increase in Bax and caspase-3 expression [35]. BDNF and NGF are well recognized to have correlational alterations of neurotrophic factors [36]. It has been discovered that NGF and BDNF were up-regulated in our study. Previous researches reveal that TNF-α and IL-6 interfere with the immune dysfunction and also affect inflammation of tissues [37]. Wilcox et al. have

proposed that the pharmacological suppression of specific proinflammatory signaling is helpful for the treatment of drug-resistant epilepsy, which could possibly delay or even prevent epileptogenesis [38].

As reported, antioxidant therapies targeting oxidative stress have received considerable attention in epilepsy treatment [39]. PTZ-induced reductions in total SOD activity and lipid antioxidant (a-tocopherol) content were observed in rat brain homogenates [40]. Meanwhile, the levels of MDA in the epilepsy patient were found to be higher compared to those of the control group [41]. These findings were consistent in our studies showing that SOD activity decreased, and MDA expression increased in the hippocampus in epilepsy. And both miR-96 mimics and RAC1 knockdown could reverse these pathologies.

At last, several studies have reported the miRNA changes in epilepsy, and we did an exosomal miRNAs chip-array from cell culture mediums. The exosomes released from these cells were confirmed by the size with NTA analysis and shape in EM. Importantly, we found the decreased expression of miR-96 in excitotoxic neurons treated with KA and this was prevented in cocultured excitotoxic neurons with astrocytes. Meanwhile, we also found the increased expression of exosomal miR-103 in KA treated neurons and this could be reversed by cocultured astrocytes as well, which is consistent with our previous study showing miR-103 is involved in the pathology of epilepsy [42].

However, in our studies, there are several limitations need to be addressed. One is the rescue study for the association between of miR-96 and Rac1 and their roles in epilepsy-related neurodegeneration. Based on the Target scan website, we found rat miR-96 has a target of 967 transcripts with conserved sites, containing a total of 1085 conserved sites and 251 poorly conserved sites. In future studies, we will design a series of rescue study to investigate the exact targets of miR-96. The other is the cell-specific changes in epilepsy. We found acute seizure rats have increased astrocytic marker GFAP and inflammatory marker (TNF−α and IL-6) in hippocampal homogenate and miR-96 mimics could reduce these pathologies. However, we did not do a further flowcytometry to separate these changes to individually compare the results in neurons, astrocytes and even microglias. It would be promising to compare these pathological markers in a single-cell profiling style. Last but not least, since the early publications [43], researchers have used the pilocarpine model to address acute seizure mechanisms and variables associated with SE attenuation, in addition to mechanisms that relate to the development and profile of chronic epilepsy in the post-SE period. The epilepsy after brain insults have been divided into two stages: acute and chronic stage. In our study, we were focusing on the pathology in acute stage which might be involved in the latency period and chronic epileptic stage.

Conclusion

In conclusion, our study revealed that upregulation of miR-96 could down-regulate RAC1 gene and inhibit the activation of RhoA/ROCK signaling pathway, thus alleviate the neurological damage in acute seizure rats. The further investigation of the cell-specific mechanism should be more scrupulously and profoundly performed with a larger cohort to provide a promising clinical application in treatment for patients with epilepsy.

Abbreviations

AEDs: antiepileptic drugs

Bax：BCL2 Associated X

Bcl-2: B-cell lymphoma 2

BDNF: brain-derived neurotrophic factor

BrdU：bromodeoxyuridine

EEG: electroencephalogram

ELISA：Enzyme-linked immunosorbent assay

EM: Electron Microscopy

GAPDH：glyceraldehyde-3-phosphate dehydrogenase

GFAP: glial fibrillary acidic protein

IL-6: interleukin-6

KA: Kainic acid

MDA: malonadialdehyde

miR: miRNA

NC: Negative control

NGF: nerve growth factor

NTA: Nanoparticle tracking analysis

RAC1: Rac Family Small GTPase 1

RhoA/ROCK: Ras Homolog Family Member A/Rho kinase (ROCK)

RNA：Ribonucleic Acid

RT-qPCR: Reverse transcription quantitative polymerase chain reaction

SE: Status epilepticus

siRNA: small interfere RNA

SOD: superoxide dismutase

TNF-α: tumor necrosis factor-α

PBS：Phosphate Buffered Saline

PTZ: Pentylenetetrazol

TLE: temporal lobe epilepsy

TUNEL：TdT-mediated dUTP Nick-End Labeling

PVDF：polyvinylidene difluoride

3'UTR：3'-untranslated region

Declarations

Ethical Approval and Consent to participate

Statement in the Methods part. Experiments were performed under ethical guidelines (20170223-001) and handled according to institutionally- approved procedures.

Consent for publication

Statement in the Cover Letter.

Availability of supporting data

The datasets supporting the conclusions of this article are available from the corresponding author.

Funding

This work was supported by Natural Science Foundation of China (Grant number: 81701231), Natural Science Foundation of Shanghai (16ZR1431500), Shanghai Pudong New Area Key Project (PWZzk2017-16)

Authors' contributions

ZP & CW conceived, designed the experiments and performed cell cultures. WZH and JW ran the animal study and molecular tests. CW & ZP did the cell culture and exosome isolation. RDB, & ZP analyzed the data and wrote the manuscript. All authors read and approved the final manuscript.

Competing interests

The authors declare that they have no competing interests.

Acknowledgements

Not applicable.

References

1. Fisher, R.S., et al., *ILAE official report: a practical clinical definition of epilepsy.* Epilepsia, 2014. **55**(4): p. 475-82.
2. Bell, G.S., A. Neligan, and J.W. Sander, *An unknown quantity--the worldwide prevalence of epilepsy.* Epilepsia, 2014. **55**(7): p. 958-62.
3. Cilio, M.R., E.A. Thiele, and O. Devinsky, *The case for assessing cannabidiol in epilepsy.* Epilepsia, 2014. **55**(6): p. 787-90.
4. Rankin-Gee, E.K., et al., *Perineuronal net degradation in epilepsy.* Epilepsia, 2015. **56**(7): p. 1124-33.

5. Berg, A.T., et al., *Revised terminology and concepts for organization of seizures and epilepsies: report of the ILAE Commission on Classification and Terminology, 2005-2009.* Epilepsia, 2010. **51**(4): p. 676-85.
6. Ekizoglu, E., et al., *Investigation of neuronal autoantibodies in two different focal epilepsy syndromes.* Epilepsia, 2014. **55**(3): p. 414-22.
7. Yan, Z., et al., *miR-96/HBP1/Wnt/beta-catenin regulatory circuitry promotes glioma growth.* FEBS Lett, 2014. **588**(17): p. 3038-46.
8. Ubhi, K., et al., *Widespread microRNA dysregulation in multiple system atrophy - disease-related alteration in miR-96.* Eur J Neurosci, 2014. **39**(6): p. 1026-41.
9. Kaalund, S.S., et al., *Aberrant expression of miR-218 and miR-204 in human mesial temporal lobe epilepsy and hippocampal sclerosis-convergence on axonal guidance.* Epilepsia, 2014. **55**(12): p. 2017-27.
10. Li, Z. and Y. Wang, *miR-96 targets SOX6 and promotes proliferation, migration, and invasion of hepatocellular carcinoma.* Biochem Cell Biol, 2018. **96**(3): p. 365-371.
11. Yamada, Y., et al., *MiR-96 and miR-183 detection in urine serve as potential tumor markers of urothelial carcinoma: correlation with stage and grade, and comparison with urinary cytology.* Cancer Sci, 2011. **102**(3): p. 522-9.
12. Wang, X.F., et al., *MicroRNAs as biomarkers in molecular diagnosis of refractory epilepsy.* Chinese Neurosurgical Journal, 2016. **2**: 28.
13. Watson, I.R., et al., *The RAC1 P29S hotspot mutation in melanoma confers resistance to pharmacological inhibition of RAF.* Cancer Res, 2014. **74**(17): p. 4845-4852.
14. Cuadrado, A., et al., *Transcription factors NRF2 and NF-kappaB are coordinated effectors of the Rho family, GTP-binding protein RAC1 during inflammation.* J Biol Chem, 2014. **289**(22): p. 15244-58.
15. Li, J., et al., *Increased Expression of Rac1 in Epilepsy Patients and Animal Models.* Neurochem Res, 2016. **41**(4): p. 836-43.
16. Fujita, Y. and T. Yamashita, *Axon growth inhibition by RhoA/ROCK in the central nervous system.* Front Neurosci, 2014. **8**: p. 338.
17. Liu, A.H., et al., *The roles of interleukin-1 and RhoA signaling pathway in rat epilepsy model treated with low-frequency electrical stimulation.* J Cell Biochem, 2018. **119**(3): p. 2535-2544.
18. Palfi, A., et al., m*icroRNA regulatory circuits in a mouse model of inherited retinal degeneration.* Sci Rep, 2016.31431.
19. Chen, W., He, B., and Zheng. P. *Astrocytic insulin-like growth factor-1 prevents excitotoic downregulation of adenosine deaminase acting on RNA in calcium dynamics.* J Cell Biochem, 2019. **120**(6): 9097-103.
20. Nowell, M., et al., *Utility of 3D multimodality imaging in the implantation of intracranial electrodes in epilepsy.* Epilepsia, 2015. **56**(3): p. 403-13.
21. Chowdhury, F.A., et al., *Impaired cognitive function in idiopathic generalized epilepsy and unaffected family members: an epilepsy endophenotype.* Epilepsia, 2014. **55**(6): p. 835-40.
22. Gan, J., et al., *An evaluation of the links between microRNA, autophagy, and epilepsy.* Rev Neurosci, 2015. **26**(2): p. 225-37.
23. Gan, J., et al., *miR-96 attenuates status acute seizureus-induced brain injury by directly targeting Atg7 and Atg16L1.* Sci Rep, 2017. **7**(1): p. 10270.
24. Feng, J., et al., *HERG1 functions as an oncogene in pancreatic cancer and is downregulated by miR-96.* Oncotarget, 2014. **5**(14): p. 5832-44.
25. Huang, X., et al., *miR96 functions as a tumor suppressor gene by targeting NUAK1 in pancreatic cancer.* Int J Mol Med, 2014. **34**(6): p. 1599-605.
26. Wang, Z., et al., *Rac1 is crucial for Ras-dependent skin tumor formation by controlling Pak1-Mek-Erk hyperactivation and hyperproliferation in vivo.* Oncogene, 2010. **29**(23): p. 3362-73.
27. Sylow, L., et al., *Rac1–a novel regulator of contraction-stimulated glucose uptake in skeletal muscle.* Exp Physiol, 2014. **99**(12): p. 1574-80.
28. Sylow, L., et al., *Akt and Rac1 signaling are jointly required for insulin-stimulated glucose uptake in skeletal muscle and downregulated in insulin resistance.* Cell Signal, 2014. **26**(2): p. 323-31.
29. Palfi A, M.-W.S., Chadderton N, et al., *MiR-182 and miR-96 co-regulate Rac1 expression in the mouse retina[J].* Investigative Ophthalmology & Visual Science, 2015. **56(7)**: p. 4672-4672.
30. El-Sibai, M., et al., *RhoA/ROCK-mediated switching between Cdc42- and Rac1-dependent protrusion in MTLn3 carcinoma cells.* Exp Cell Res, 2008. **314**(7): p. 1540-52.
31. Mead, T.J. and V. Lefebvre, *Proliferation assays (BrdU and EdU) on skeletal tissue sections.* Methods Mol Biol, 2014. **1130**: p. 233-243.
32. Bartley, J., et al., *BrdU-positive cells in the neonatal mouse hippocampus following hypoxic-ischemic brain injury.* BMC Neurosci, 2005. **6**: p. 15.
33. Lindqvist, L.M., et al., *Prosurvival Bcl-2 family members affect autophagy only indirectly, by inhibiting Bax and Bak.* Proc Natl Acad Sci U S A, 2014. **111**(23): p. 8512-7.
34. Erturk, A., Y. Wang, and M. Sheng, *Local pruning of dendrites and spines by caspase-3-dependent and proteasome-limited mechanisms.* J Neurosci, 2014. **34**(5): p. 1672-88.
35. Mikati, M.A., et al., *Changes in sphingomyelinases, ceramide, Bax, Bcl(2), and caspase-3 during and after experimental status epilepticus.* Epilepsy Res, 2008. **81**(2-3): p. 161-6.
36. Budni, J., et al., *The involvement of BDNF, NGF and GDNF in aging and Alzheimer's disease.* Aging Dis, 2015. **6**(5): p. 331-41.
37. Umare, V., et al., *Effect of proinflammatory cytokines (IL-6, TNF-alpha, and IL-1beta) on clinical manifestations in Indian SLE patients.* Mediators Inflamm, 2014. **2014**: p. 385297.
38. Wilcox, K.S. and A. Vezzani, *Does brain inflammation mediate pathological outcomes in epilepsy?* Adv Exp Med Biol, 2014. **813**: p. 169-83.
39. Shina, E.J., et al. *Role of oxidative stress in epileptic seizures.* Neurochem Int, 2011. **59**(2): 122–37.

40. Rauca, C., et al. *The role of superoxide dismutase and alpha-tocopherol in the development of seizures and kindling induced by pentylenetetrazol - influence of the radical scavenger alpha-phenyl-N-tert-butyl nitrone.* Brain Res, 2004. **1009**(1-2):203-12.
41. Nilüfer, D.,et al. *Investigation of PON1 activity and MDA levels in patients with epilepsy not receiving antiepileptic treatment.* Neuropsychiatr Dis Treat, 2016; **12**: 1013–7.
42. Zheng, P., et al. *Inhibition of microRNA-103a inhibits the activation of astrocytes in hippocampus tissues and improves the pathological injury of neurons of epilepsy rats by regulating BDNF.* Cancer Cell Int, 2019. **19**:109
43. Turski, W.A., et al. *Seizures produced by pilocarpine in mice: a behavioral, electroencephalographic and morphological analysis.* Brain, 1984. **321**:237-53.

Figures

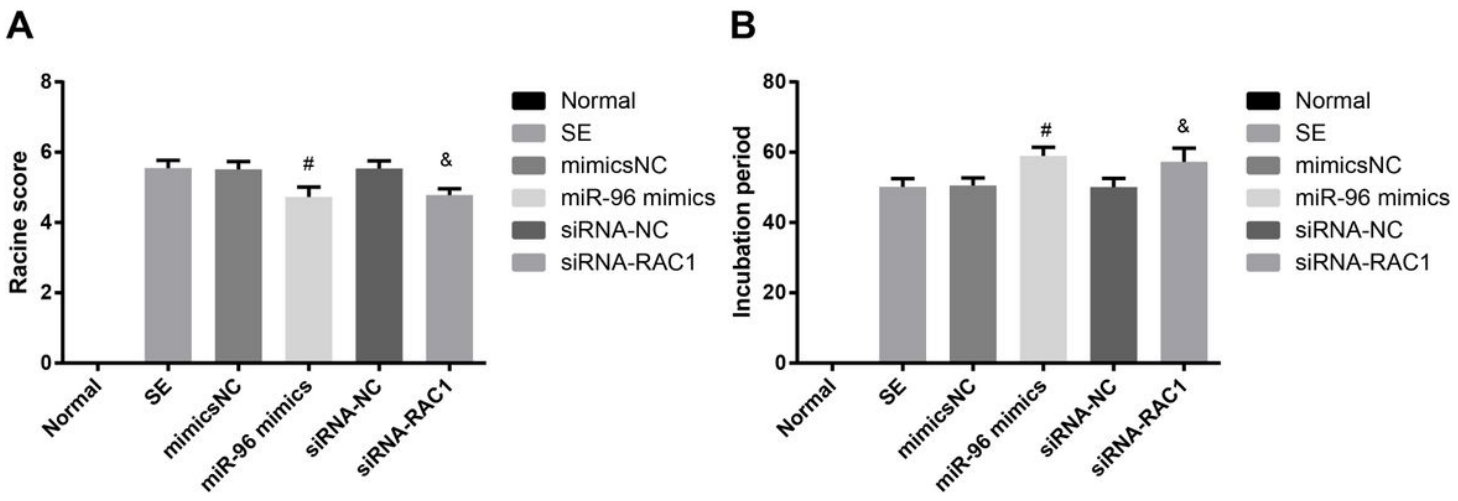

Figure 1

Racine score is reduced and latency of epilepsy is prolonged by upregulated miR-96 or decreased RAC1 in acute seizure rats. A: Racine score of SD rats of each group; B: Comparison of latency period in each group of rats. The data was in the form of mean ± standard deviation. One-way ANOVA was used for comparison among groups. LSD-t test was used for pairwise comparison, N = 12 in each group, # $P < 0.05$ compared to the mimics NC group; & $P < 0.05$ compared with the siRNA-NC group.

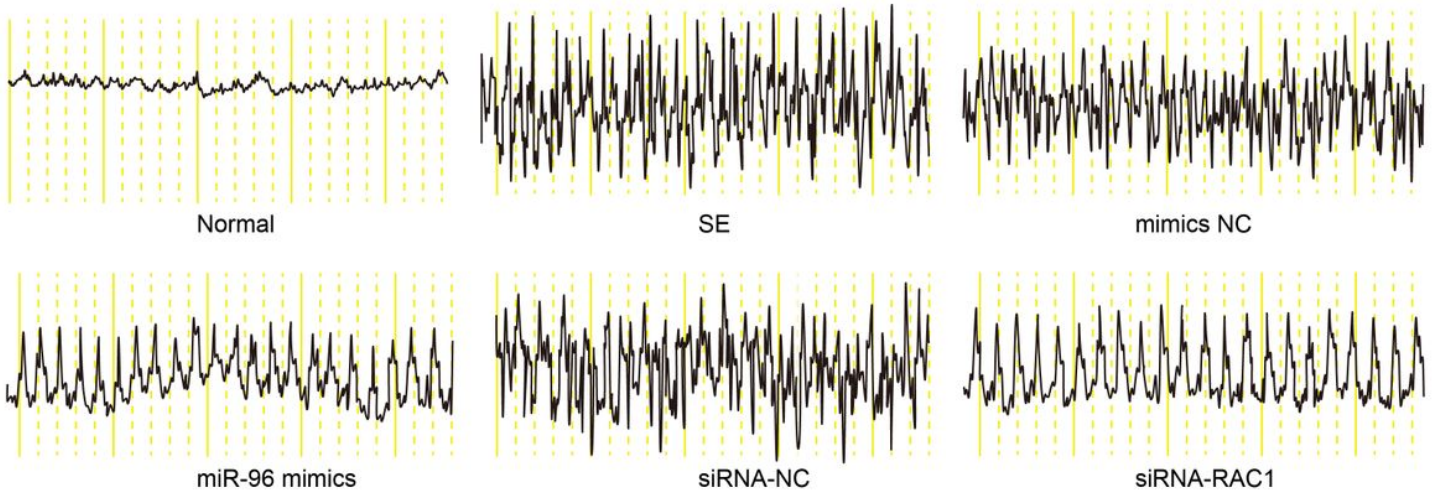

Figure 2

The amplitude of spike wave and frequency of EEG is reduced by upregulated miR-96 or decreased RAC1. Paper is recorded at 30mm/s.

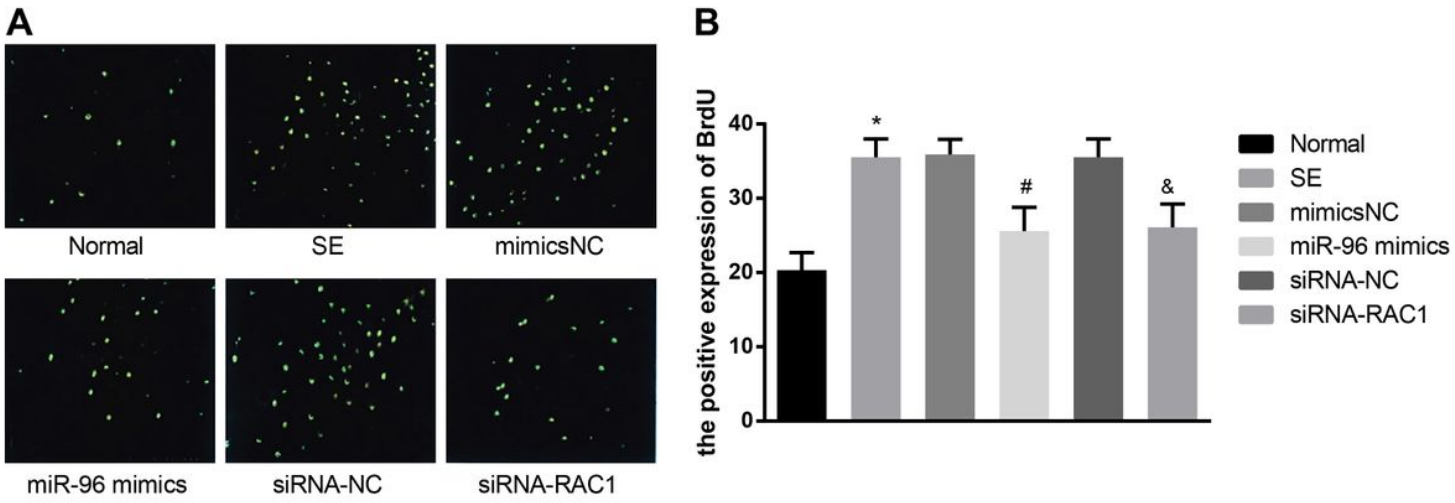

Figure 3

BrdU-positive cell is dramatically reduced by upregulated miR-96 or decreased RAC1. A: Expression of BrdU-positive cells in hippocampal tissues by immunofluorescence staining; B: Quantification results of BrdU-positive cells in Fig. A. The data in the figure were in the form of mean ± standard deviation. One-way ANOVA was used for comparison among groups. LSD-t test was used for pairwise comparison after ANOVA analysis, N = 3. * compared with the normal group, P < 0.05; # compared with the mimics NC group, P < 0.05; & compared with the siRNA-NC group, P < 0.05.

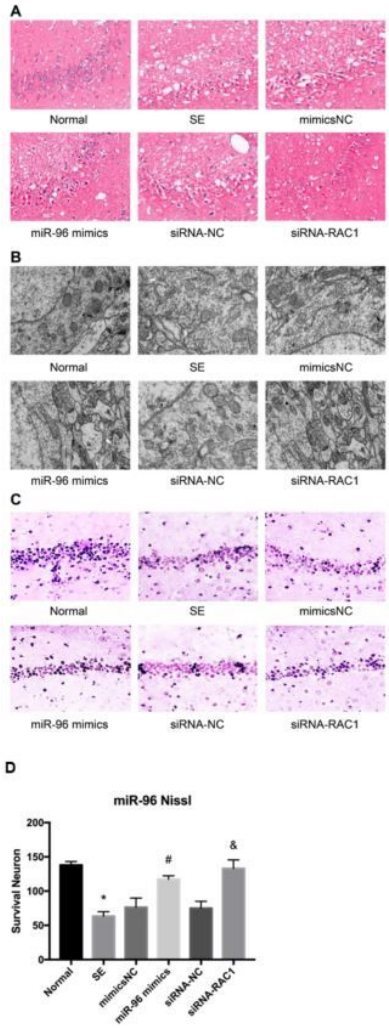

Figure 4

The pathological changes of hippocampus in acute seizure rats are recovered by upregulated miR-96 and decreased RAC1. A: HE staining of hippocampus of SD rats in each group; B: Electron microscopic observation of hippocampus of SD rats in each group; C: Nissl's staining of hippocampus of SD rats in each

group. D: Quantification of Nissl's staining of hippocampal neurons in each group.

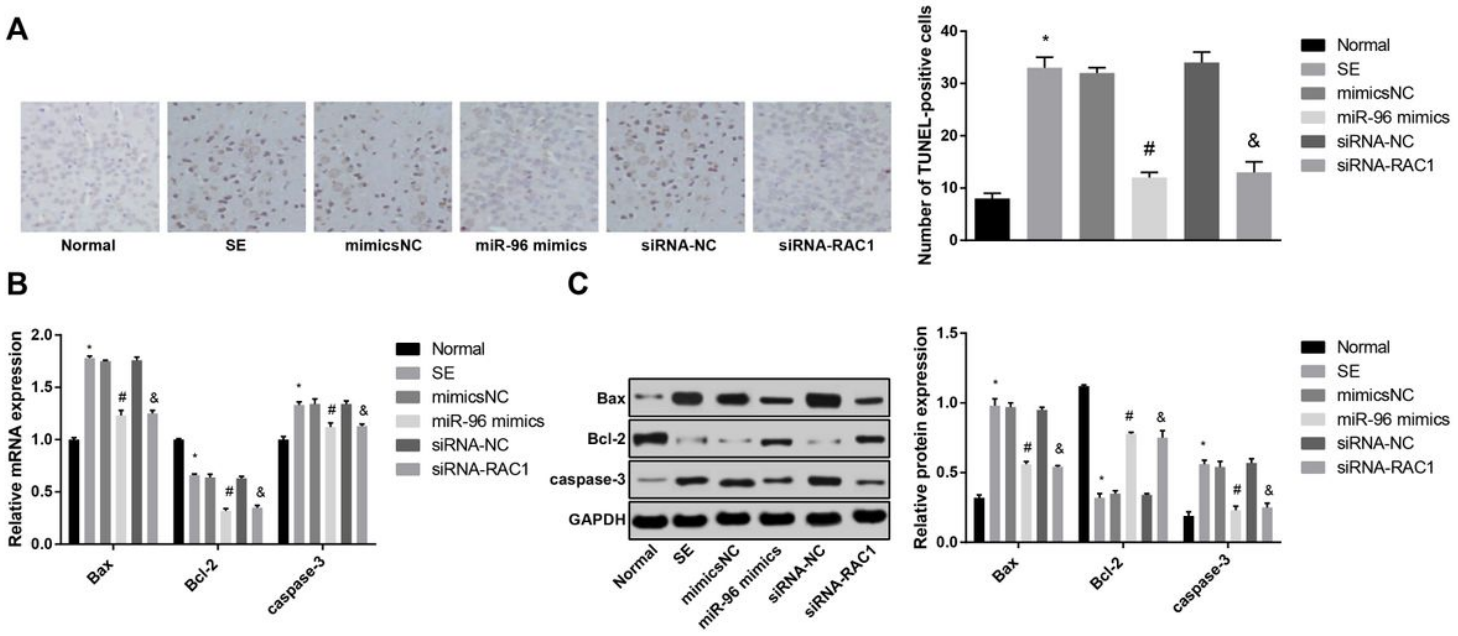

Figure 5

TUNEL-positive cell is reduced, Bax and caspase-3 expression is inhibited, and Bcl-2 expression is promoted by upregulated miR-96 or decreased RAC1. A: Positive expression of apoptotic cells and positive cells in hippocampus by TUNEL staining; B: The mRNA expression of Bax, caspase-3 and Bcl-2 in RT-qPCR; C: The protein expression of Bax, caspase-3, and Bcl-2 in western blot analysis. The data were in the form of mean ± standard deviation. One-way ANOVA was used for comparison among groups. LSD-t test was used for pairwise comparison after ANOVA analysis, N = 10. * compared with the normal group, P < 0.05; # compared with the mimics NC group, P < 0.05; & compared with the siRNA-NC group, P < 0.05.

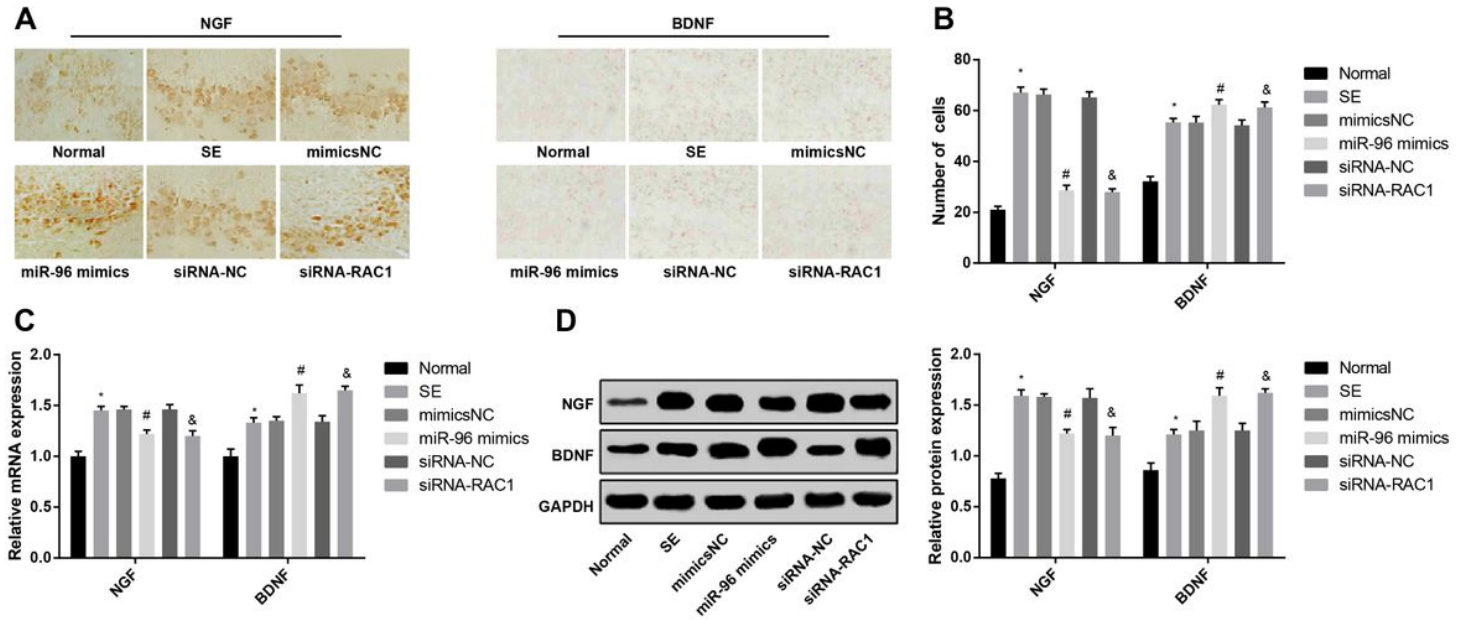

Figure 6

NGF is inhibited and BDNF is promoted by upregulated miR-96 or decreased RAC1. A: Immunohistochemical staining for positive expression of NGF and BDNF in hippocampus; B: Quantification results of positive expression of NGF and BDNF in Fig. A; C: The mRNA expression of NGF and BDNF in RT-qPCR. D: The protein expression of NGF and BDNF in western blot analysis; the data were shown as the mean ± standard deviation form. One-way ANOVA was used for comparison among groups. LSD-t test was used for pairwise comparison after ANOVA analysis, N = 10. * compared with the normal group, P < 0.05; # compared with the mimics NC group, P < 0.05; & compared with the siRNA-NC group, P < 0.05.

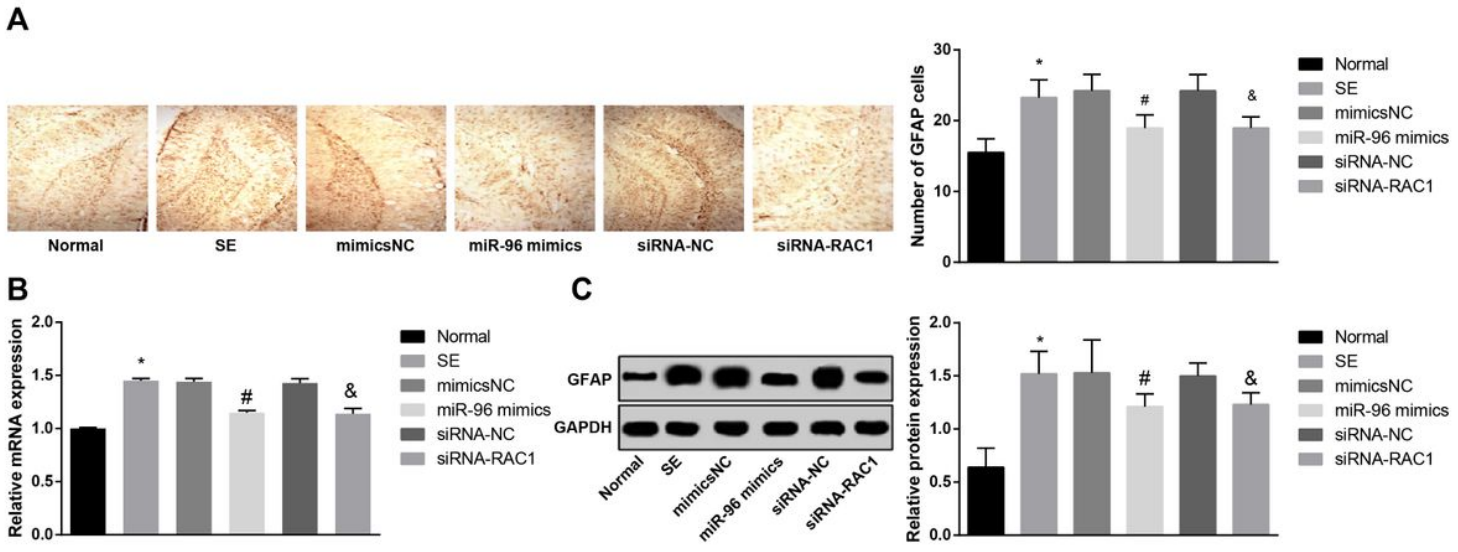

Figure 7

The expression of GFAP is inhibited by upregulated miR-96 or decreased RAC1. A: Expression of GFAP-positive cells in hippocampus by immunohistochemical staining; B: The mRNA expression of GFAP in RT-qPCR; C: GFAP protein expression in western blot analysis. The data were in the form of mean ± standard deviation. One-way ANOVA analysis of variance was used for comparison among groups. LSD-t test was used for pairwise comparison after ANOVA analysis, N = 10. * compared with the normal group, P < 0.05; # compared with the mimics NC group, P < 0.05; & compared with the siRNA-NC group, P < 0.05.

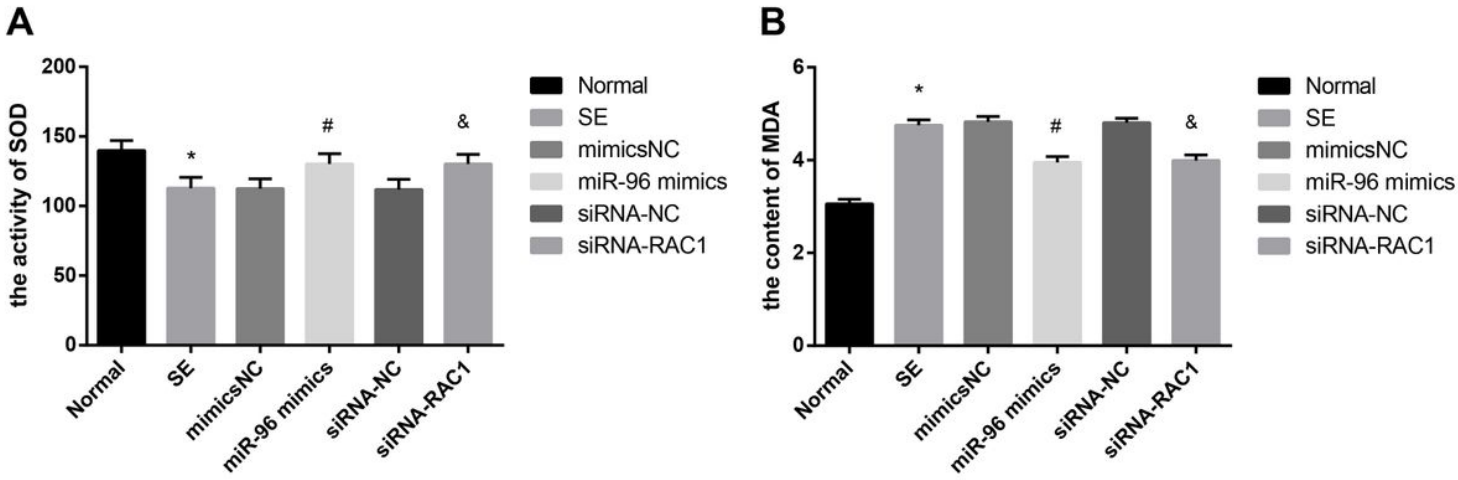

Figure 8

SOD activity is increased and MDA content decreased by upregulated miR-96 and decreased RAC1. A: SOD activity in hippocampus of each group of rats; B: Expression of MDA in hippocampus of each group of rats. The data were in the form of mean ± standard deviation. One-way ANOVA was used for comparison among multiple groups. LSD-t test was used for pairwise comparison after ANOVA analysis, N = 10. * compared with the normal group, P < 0.05; # compared with the mimics NC group, P < 0.05; & compared with the siRNA-NC group, P < 0.05.

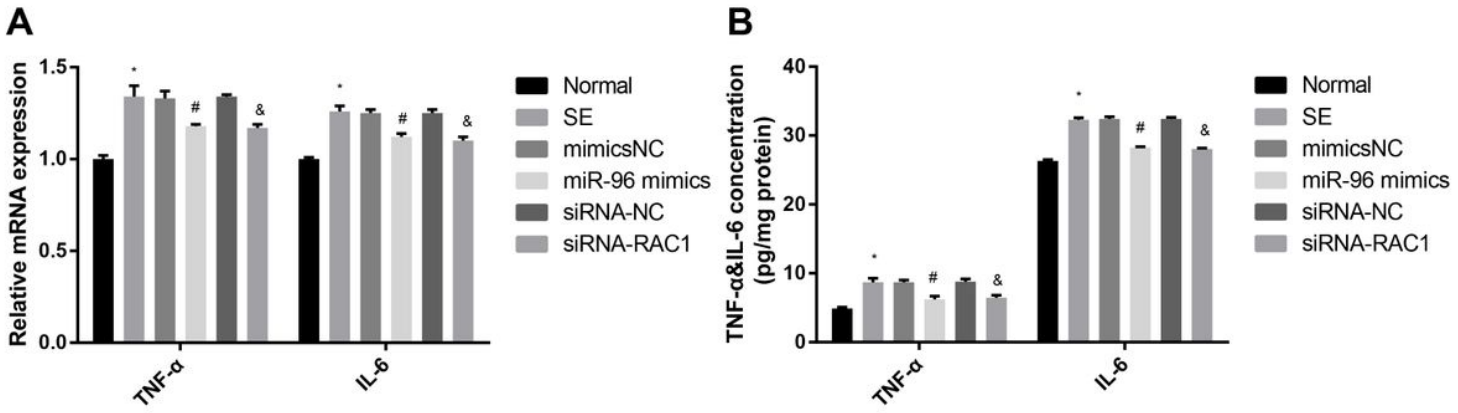

Figure 9

TNF-α and IL-6 expression levels are inhibited by upregulated miR-96 or decreased RAC1. A: expression of TNF-α and IL-6 mRNA in hippocampus of each group; B: Protein expression of TNF-α and IL-6 in hippocampus of each group. The data were in the form of mean ± standard deviation. One-way ANOVA was used for comparison among multiple groups. LSD-t test was used for pairwise comparison after ANOVA analysis, N = 10. * compared with the normal group, P < 0.05; # compared with the mimics NC group, P < 0.05; & compared with the siRNA-NC group, P < 0.05.

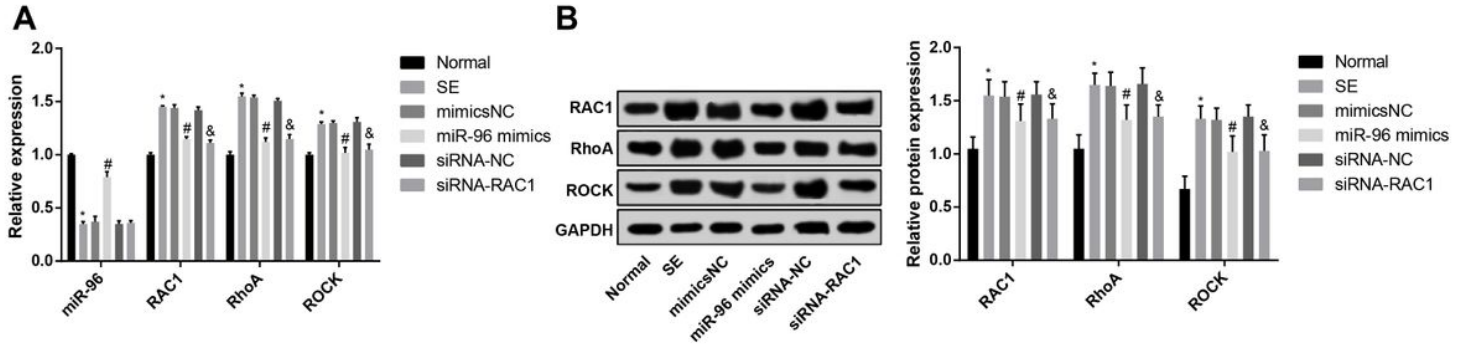

Figure 10

RhoA and ROCK expression levels are inhibited by upregulated miR-96 or decreased RAC1. A: RNA level of miR-96, RAC1, RhoA, and ROCK in RT-qPCR; B: Protein expression of RAC1, RhoA, and ROCK in western blot analysis. The data were in the form of mean ± standard deviation. One-way ANOVA was used for comparison among multiple groups. LSD-t test was used for pairwise comparison after ANOVA analysis, N = 10. * compared with the normal group, P < 0.05; # compared with the mimics NC group, P < 0.05; & compared with the siRNA-NC group, P < 0.05.

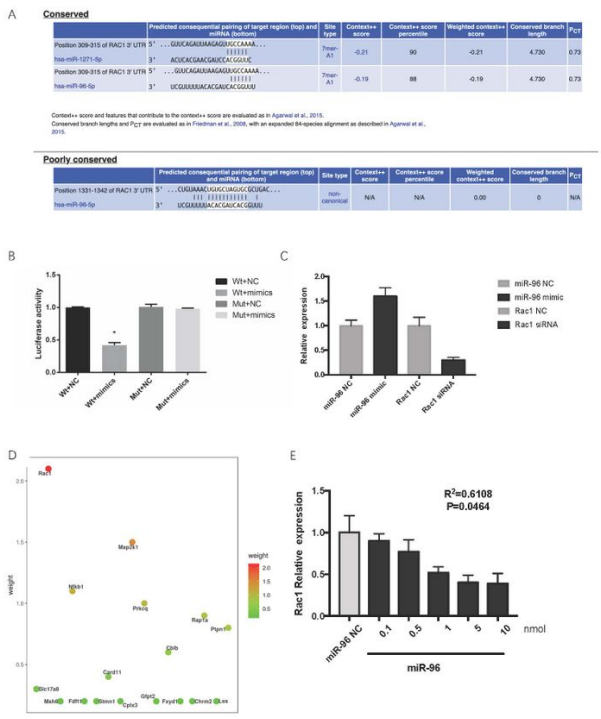

Figure 11

RAC1 is the direct target gene of miR-96. A: Target Scan predicts the target site for RAC1 binding to the corresponding miR-96. B: Detection results of dual luciferase reporter gene activity. C: After treating neurons with miR-96 mimic or Rac1 siRNA, the expression of miR-96 was upregulated and the Rac1 was downregulated. D: The top 10 target genes of miR-96 were listed based on their weight in Bubble figure. E: The dose-dependent relationship between miR-96 mimic and relative expression of Rac1 with R2=0.6108 and P <0.05. Data represents the mean ± standard deviation of three independent experiments. * P < 0.05 compared with the Wt + NC group.

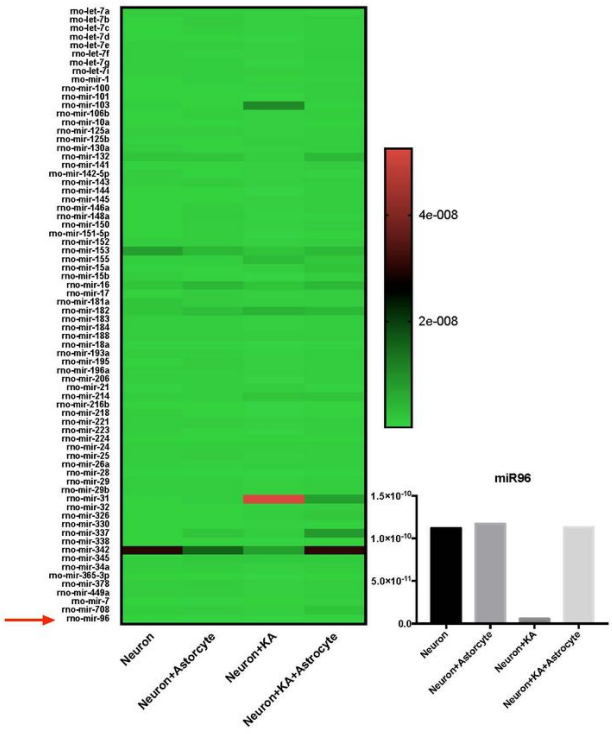

Figure 12

The heat map demonstrates the miRNA alterations in exosomes from primary cultured neurons, neurons cocultured with astrocytes, KA treated neurons and KA treated neurons cocultured with astrocytes. The expression of miR-96, which was decreased in KA treated neurons and the co-cultured astrocytes could increase its expression.

Supplementary Files

This is a list of supplementary files associated with this preprint. Click to download.

- NTAmiRNA.docx
- TableS2ExosomalmiRNAs.docx
- tableS1.docx